

Multidimensional Wavelet Analysis of Geophysical Monitoring Time Series

A. A. Lyubushin, Jr.

*Schmidt United Institute of Physics of the Earth, Russian Academy of Sciences,
Bol'shaya Gruzinskaya ul. 10, Moscow, 123810 Russia*

Received April 24, 2000

Abstract—A method for the analysis of low-frequency geophysical monitoring time series based on the concept of the wavelet-aggregated signal previously introduced by the author is proposed. The goal of this study is the recognition of the time intervals during which the intensity of small-scale variations synchronously occurring in all time series increases. A similar problem was previously studied by the author when searching for fast spectral variations (disarrangement) in the high-frequency component of a given signal simultaneously present in all time series analyzed. This common signal was previously extracted from the aggregated signal constructed on the basis of the classic Fourier transform of the initial time series, and the time moments of the disarrangement discovered in low-frequency monitoring problems were called "slow events" by analogy with slow earthquakes. Such anomalies can indicate motions on block boundaries and fracture of the crustal material and are relevant to the search for critical geophysical phenomena. Based on the joint processing of variations in the groundwater level measured in four aquifers in the Moscow region during the period from 1993 through 1997, this paper addresses the application of orthogonal wavelets as compared with the ordinary Fourier basis.

INTRODUCTION

This study analyzes data from low-frequency geophysical monitoring systems that yield time series of various types and scales reflecting changes in various geophysical parameters or in a single parameter measured at various points. Lyubushin [1993, 1994, 1998a, 1999] proposed and developed methods for the analysis of such multidimensional time series. These methods allow the recognition of synchronization signals (specified by frequency bands and time intervals) from time series of various geophysical fields by estimating the evolution of the eigenvalues of spectral matrices and canonical coherencies in a moving time window (peaks in these statistics are associated with synchronization signals).

Lyubushin [1998b] proposed the notion of an aggregated signal, which is a scalar signal providing maximum information on the most general variations present in all of the processes analyzed and at the same time suppressing components that are characteristic of individual processes and usually represent local noise caused by specific measurement conditions, anthropogenic factors, or measurement uncertainties. The aggregated signal is constructed in two stages. At the first stage, the initial multidimensional series is converted to a multidimensional series of the so-called canonical components that preserve common signals and are free from local ones. At the second stage, the common signals are additionally amplified by constructing a scalar series, which is their first main component and is called an aggregated signal of the initial multidimensional time series. Each stage of the aggregation procedure is

implemented as a sequence of projections of multidimensional Fourier transforms onto eigenvectors of various spectral matrices. Lyubushin [1998b, 1999] and Lyubushin *et al.*, [1999] applied the Fourier-aggregated signal to the search for earthquake precursors and to the study of the fine structure of multidimensional geophysical time series.

Lyubushin [2000] generalized the construction of the aggregated signal by using, instead of the Fourier expansion of time series, the expansion in the complete orthogonal system of compactly supported functions (wavelets) and introduced the notion of a wavelet-aggregated signal. The latter enables the analysis of strongly nonstationary and non-Gaussian time series to which Fourier methods are applicable but insufficiently effective. In particular, a short-term precursor was identified in the case study of the strongest Tien Shan earthquake in China ($M = 7.8$, July 28, 1976) [Lyubushin, 2000].

The goal of this study is to develop a method for determining the lifetime of short-lived anomalies that synchronously occur in all time series. Such anomalies can indicate motion processes on block boundaries and fracture of the crustal material; they also can be useful in studies of critical geophysical phenomena. The method uses the wavelet-aggregated signal which, upon a sequence of nonlinear filtering procedures, serves as a basis for constructing a sequence of critical time intervals of the most drastic changes in the aggregated signal.

The method is illustrated with a case study of groundwater level variations measured in four aquifers

in the Moscow region during 1993–1997. The results are compared with anomalies obtained from the same data using the recognition algorithm of slow events [Lyubushin *et al.*, 1999].

METHOD

The orthogonal multiresolution analysis (wavelet expansion) of a signal $x(t)$ is defined by the expression [Chui, 1992; Daubechies, 1988, 1992]

$$x(t) = \sum_{\alpha=-\infty}^{+\infty} x^{(\alpha)}(t), \tag{1}$$

$$x^{(\alpha)}(t) = \sum_{j=-\infty}^{+\infty} c^{(\alpha)}(\tau_j^{(\alpha)}) \Psi^{(\alpha)}(t - \tau_j^{(\alpha)}), \quad \tau_j^{(\alpha)} = j \times 2^\alpha.$$

Here, α is the number of the detail level, and

$$c^{(\alpha)}(\tau_j^{(\alpha)}) = \int_{-\infty}^{+\infty} x(t) \Psi^{(\alpha)}(t - \tau_j^{(\alpha)}) dt \tag{2}$$

are the wavelet coefficients at the α th detail level at a time moment $\tau_j^{(\alpha)}$, and $\Psi^{(\alpha)}(t)$ are basis functions at the α th level obtained by the stretching and translation of the main wavelet function $\Psi(t)$:

$$\begin{aligned} \Psi^{(\alpha)}(t) &= (\sqrt{2})^{-\alpha} \Psi(2^{-\alpha}t), \\ \Psi^{(\alpha)}(t - \tau_j^{(\alpha)}) &= (\sqrt{2})^{-\alpha} \Psi(2^{-\alpha}t - j). \end{aligned} \tag{3}$$

The function $\Psi(t)$ is constructed so that it should be finite and have a unit norm in $L_2(-\infty, +\infty)$, and the infinite set of functions $\{\Psi^{(\alpha)}(t - \tau_j^{(\alpha)})\}$ (copies of the main wavelet translated to the points $\tau_j^{(\alpha)}$ and stretched by a factor of 2^α) should form an orthonormal basis in $L_2(-\infty, +\infty)$. For example, if

$$\begin{aligned} \Psi(t) &= -1 \quad \text{if } t \in \left(0, \frac{1}{2}\right] \\ &+1 \quad \text{if } t \in \left(\frac{1}{2}, 1\right] \\ &0 \quad \text{for other } t, \end{aligned} \tag{4}$$

Eq. (1) is the expansion of $x(t)$ in Haar wavelets. Function (4) is the simplest and most compact orthogonal finite wavelet. A well-known family of orthogonal wavelet functions is represented by Daubechies functions of even orders [Chui, 1992; Daubechies, 1988, 1992]; in addition to being finite, they nullify some of the first moments. The greater the wavelet order, the larger is the number of vanishing moments and the more extensive is the carrier.

Below, only Haar wavelets (4) are used. This choice is dictated by the fact that I seek the most pronounced common variations for which basis (4) is best suited.

Besides, the Haar basis is, to the largest degree, an “antipode” of the Fourier basis, and its application is methodologically interesting in the context of comparison with results obtained with the use of orthogonal harmonics.

Let $x(t)$ be a signal with a discrete time t N samples long, $t = t_j = j\Delta t, j = 1, \dots, N$. I assume that N is an integer of the 2^m type, which is convenient for the subsequent use of the fast wavelet transformation. If N is not equal to 2^m , the signal $x(t)$ can be complemented by zeros until its length becomes 2^m , where m is the minimum integer for which $N \leq 2^m$. In the case of a finite sample and discrete time, the formula of the multiresolution analysis is

$$\begin{aligned} x(t) &= d + \sum_{\alpha=1}^m x^{(\alpha)}(t), \\ x^{(\alpha)}(t) &= \sum_{j=1}^{2^{(m-\alpha)}} c^{(\alpha)}(\tau_j^{(\alpha)}) \Psi^{(\alpha)}(t - \tau_j^{(\alpha)}), \\ \tau_j^{(\alpha)} &= j \times 2^\alpha \Delta t. \end{aligned} \tag{5}$$

The smallest detail level is the first one, and the total number of detail levels m depends on the length of a sample. The coefficient d in (5) is equal to the mean of $x(t), t = 1, \dots, N$. The set of values $c^{(\alpha)}(\tau_j^{(\alpha)})$ and d are calculated using the direct fast wavelet transformation [Press *et al.*, 1996]. These values uniquely determine the initial sample $x(t)$, which can be reconstructed from given $c^{(\alpha)}(\tau_j^{(\alpha)})$ and d using the inverse fast wavelet transformation.

A nonlinear operation frequently used in the wavelet analysis is the so-called shrinkage:

$$\begin{aligned} \text{if } |c^{(\alpha)}(\tau_j^{(\alpha)})| \leq h, \quad \text{then } c^{(\alpha)}(\tau_j^{(\alpha)}) &= 0; \\ \text{otherwise, } c^{(\alpha)}(\tau_j^{(\alpha)}) &\text{ is unchanged,} \end{aligned} \tag{6}$$

where the threshold h is chosen as a γ -quantile of the empirical function of the distribution $F_{\text{emp}}(c)$ of all wavelet coefficient moduli $|c^{(\alpha)}(\tau_j^{(\alpha)})|$ at all detail levels and at all time moments

$$F_{\text{emp}}(h) = \gamma, \quad 0 < \gamma < 1. \tag{7}$$

Usually, $\gamma = 0.95-0.999$; i.e., only 0.1–5% of the largest (in modulus) coefficients remain unchanged, and the others vanish. Upon applying operation (6), the inverse fast wavelet transformation of the new coefficients is performed. These operations produce a new signal that is characterized by significantly lower noise and preserves the most informative variations (irrespective of the detail level number, i.e., of the period) whose form is determined by the wavelet used.

The further analysis of time series employs the wavelet-aggregated signal proposed in relation to the

search for earthquake precursors in [Lyubushin, 2000] and briefly described below. The wavelet-aggregated signal is constructed in two stages similar to the case of the Fourier expansion [Lyubushin, 1998b].

The first stage initially involves the calculation of the wavelet coefficients for each time series under study and at each scale level using the fast discrete wavelet transformation. Before the transformation, the time series are converted to series in increments and are normalized in order to provide for the joint processing of diverse physical signals of different scales. The initial wavelet coefficients are then converted to the so-called canonical wavelet coefficients. The latter are obtained from covariance matrices of wavelet coefficients at each detail level using the method of canonical correlations. This conversion aims at removing individual noise (specific of only an individual series) from the wavelet coefficients and to amplify the common component. This procedure accomplishes the first stage.

At the second stage, the intensity of the common component is additionally increased by calculating the first main component of the covariance matrices of canonical wavelet coefficients at each detail level. Thus, a scalar sequence of hypothetical wavelet coefficients is obtained at each detail level, which makes it possible to calculate the inverse discrete fast wavelet transform and to obtain the time realization of a scalar signal called the wavelet-aggregated signal of the initial time series. Since sample estimates of the covariance matrices are used, I introduce an algorithm parameter L_{\min} (representativity threshold) determining the minimum possible number of wavelet coefficients at a detail level corresponding to the time window width that can be used for sample estimation of the covariance matrix. The total number of coefficients decreases twofold as the number of the detail level increases (see Eq. (5)); therefore, the aggregation can only be carried out for several first detail levels whose number depends on the window width and representativity threshold. Below, I use the time window (the so-called adaptation window [Lyubushin, 2000]) whose width is equal to the total length of the time series in question and the value $L_{\min} = 10$.

Thus, the wavelet-aggregated signal constructed with the use of the Haar basis function (4) is the sum of general steplike variations in the initial series at all detail levels. Note that the aggregated signal has no physical dimension because it naturally generalizes variations of the same type in several time series, each possibly having its own physical dimension and being constructed after the preliminary normalization of initial data.

The next step in the method proposed is the application of the shrinkage procedure (6)–(7) to the aggregated signal with the parameter γ sufficiently close to unity. Below, the following modification of the shrinkage procedure is used. First, all wavelet coefficients corresponding to the last, largest-scale detail levels

were set equal to zero. This step is necessary because the fine high-frequency (small-scale) structure of the common signal is studied here. Procedure (6) was then individually applied to each of the remaining detail levels. The aim of this independent shrinkage is as follows. Certain scale levels are often predominant in signals and concentrate most energy. In time series of geophysical monitoring, the larger is the scale of the detail level, the higher is its amplitude. Therefore, shrinkage procedure (6) applied to the total set of coefficients is often oriented mainly toward high-amplitude variations and thereby ignores characteristics at small-scale detail levels. The modified shrinkage procedure yields only the most informative variations in the aggregated signal, with their form being determined by the basis wavelet function independently at each detail level.

The signal obtained by the nonlinear wavelet filtering procedure described above contains long intervals of zero values alternating with short pulses. Time intervals concentrating such pulses are the sought-for anomalous time intervals.

DATA PROCESSING CASE STUDY

The method was applied to long-term high-precision observations of groundwater level variations in a group of four aquifers in the Moscow region. These data were previously analyzed by Lyubushin *et al.* [1997, 1999]. Figure 1 shows results of synchronous measurements of atmospheric pressure, air temperature, and variations in the groundwater level in the aquifers at depths of 120, 180, 400, and 1000 m. Processed was the observation interval from 12:00, February 2, 1993 through 03:00, August 31, 1997 (local winter time); each of the resulting series had a length of 40096 1-hour samples. The measurements were carried out by V.A. Malugin and O.S. Kazantseva (United Institute of Physics of the Earth, Russian Academy of Sciences) at two points 40 km apart: in Moscow (Central Institute of Traumatology and Orthopedics (CITO), near the Voikovskaya subway station) and in the Moscow region (Zelenyi settlement, Noginsk district). At the first point, the level variations were measured in wells at depths of 400 and 1000 m and, at the second point, at depths of 120 and 180 m. Below, these aquifers and the related time series are denoted as “120,” “180,” “400,” and “1000” for simplicity. Variations at levels 120 and 180 are contaminated by intense cultural noise due to the water withdrawal for towns of the Moscow region. However, such noise is specific to each time series and is removed during the aggregation procedure, as mentioned above.

Figure 1 plots the CITO air temperature (Fig. 1a); CITO atmospheric pressure (Fig. 1b); initial variations in groundwater levels of aquifers 120, 180, 400, and 1000 (Figs. 1c to 1f); and groundwater variations in aquifers 120 and 400 with compensated effects of atmospheric pressure (c1) and temperature (e1). The

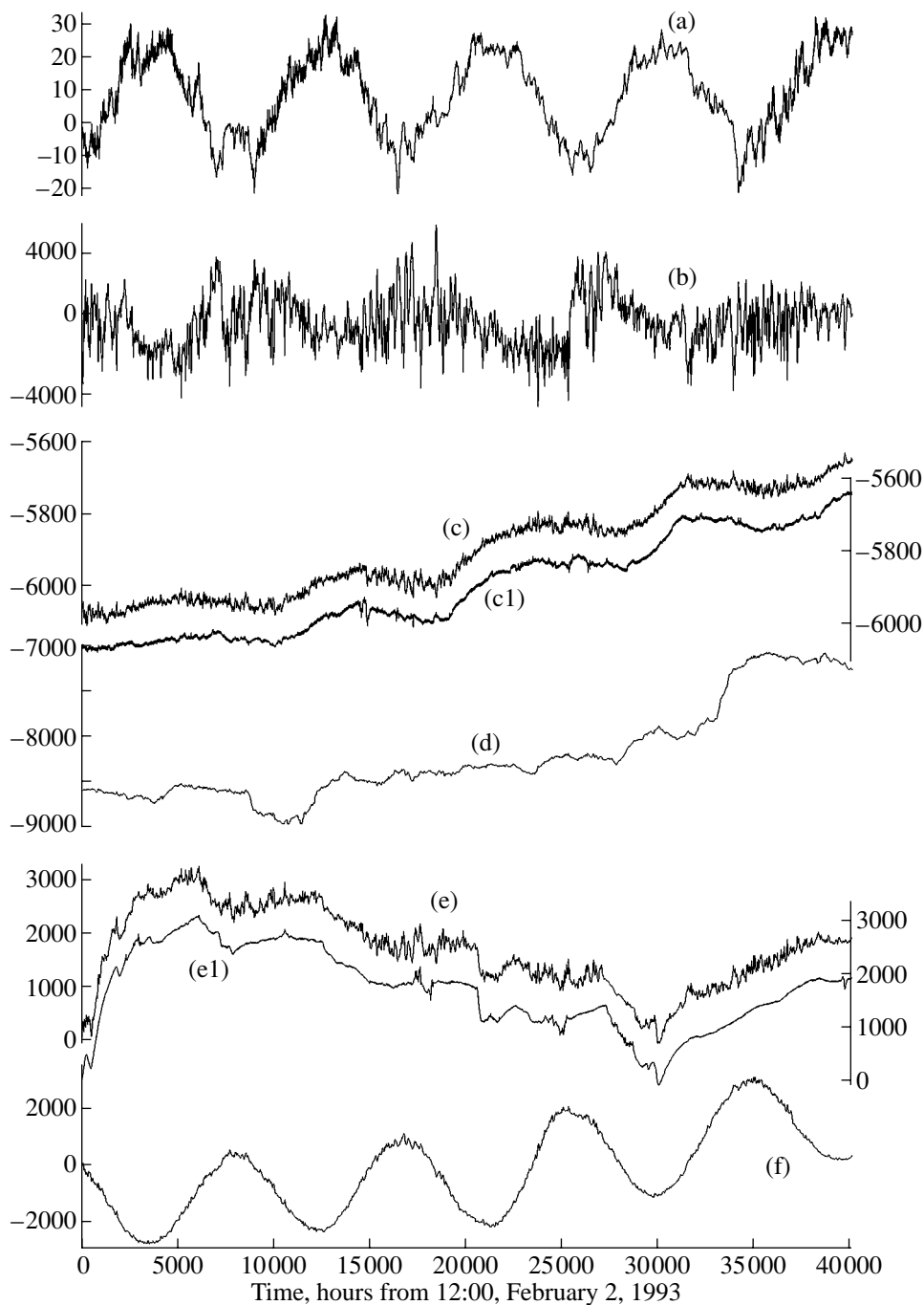


Fig. 1. Plots of time series: (a) air temperature ($^{\circ}\text{C}$); (b) atmospheric pressure (Pa) at the CITO point; (c–f) initial variations in the groundwater level (mm of water column) in the respective aquifers 120, 180, 400, and 1000; (c1) and (e1) groundwater level variations in aquifers 120 and 400 after the compensation for the effects of atmospheric pressure and temperature.

compensation procedure was applied to all groundwater level variations using the algorithm described in [Lyubushin, 1993] with a time window equal in width to the length of the total sample available. However, the compensated level plots are only given for aquifers 120 and 400 to demonstrate the behavior of the compensated time series.

These data, although with observations ended at 23:00, December 30, 1996, were analyzed in [Lyubushin *et al.*, 1999] using the technique of Fourier-aggregated signals for the recognition of slow events. The slow event was defined as a pulse in the nonstationarity measure of the high-frequency component of the Fourier-aggregated signal. The nonstationarity measure

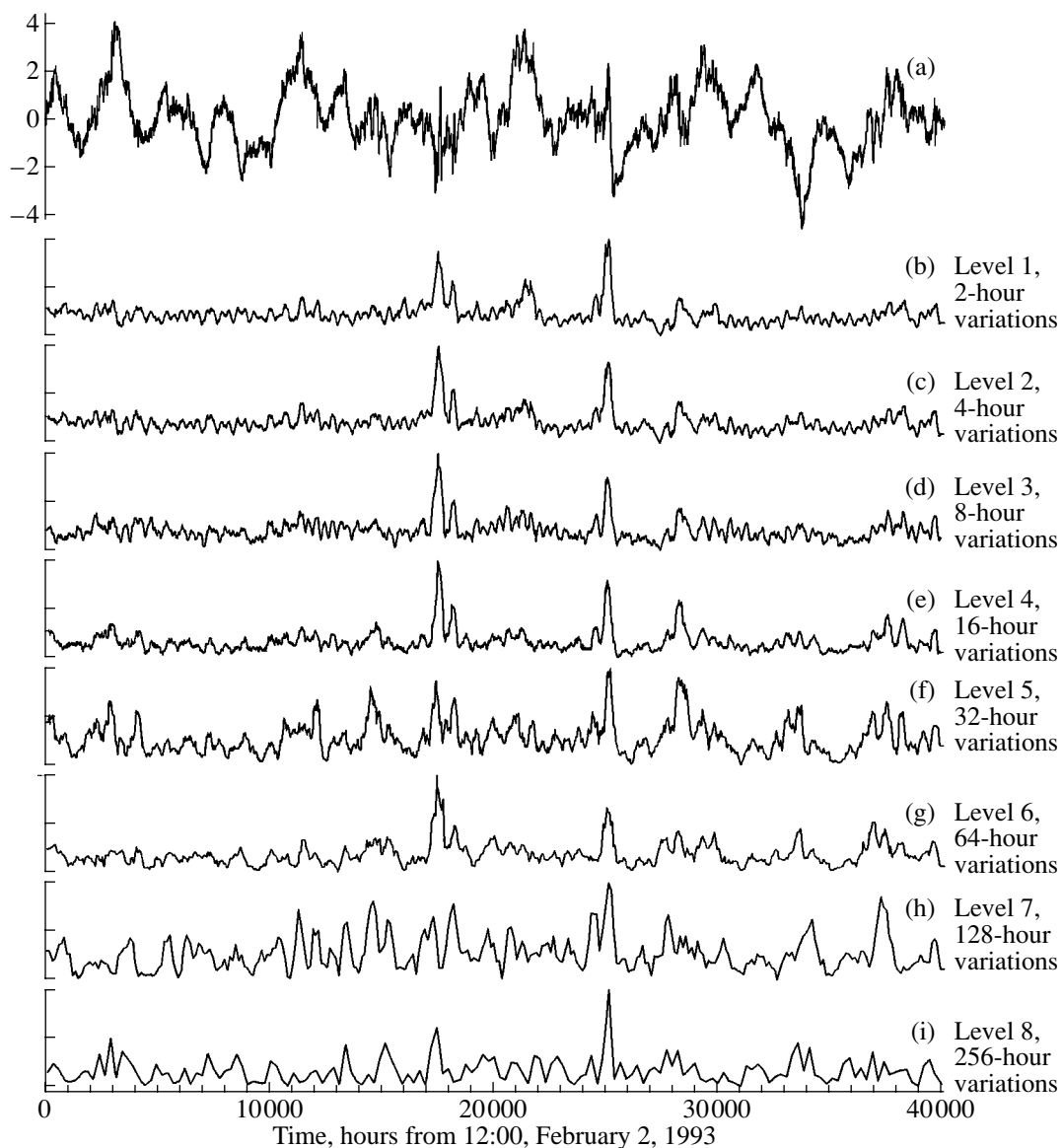


Fig. 2. Plots of (a) the wavelet-aggregated signal and (b–i) moduli of the wavelet coefficients at the initial eight detail levels of its multiresolution analysis after averaging over a time window of a 128-hour radius.

was estimated with a double moving time window and was, in essence, the difference between the coefficients of the signal autoregression model estimated to the left and right of the window center in the metric specified by the Fisher information matrix (the matrix of second derivatives of the logarithmic likelihood function) divided by the window width.

The wavelet-aggregated signal of four time series of compensated groundwater level variations is plotted in Fig. 2a. Absolute values of the wavelet coefficients are plotted in Figs. 2b–2i for the first eight detail levels of the multiresolution analysis of the aggregated signal.

The ordinate scales are different, providing maximum clearness of the variations in coefficients.

The plots of the variations in absolute values of the wavelet coefficients $|c^{(\alpha)}(\tau_j^{(\alpha)})|$ as a function of the time $\tau_j^{(\alpha)}$ provide constraints on the specific features of the signal behavior (the onset time τ and detail level α , i.e., the “period” and characteristic scale of the anomaly). Note that, if the total number of samples in a series is large, the variation plots of wavelet coefficients are very irregular at low detail levels (first values of the index α), and it is appropriate to average them in a given moving window of radius τ_{av} (similar to the aver-

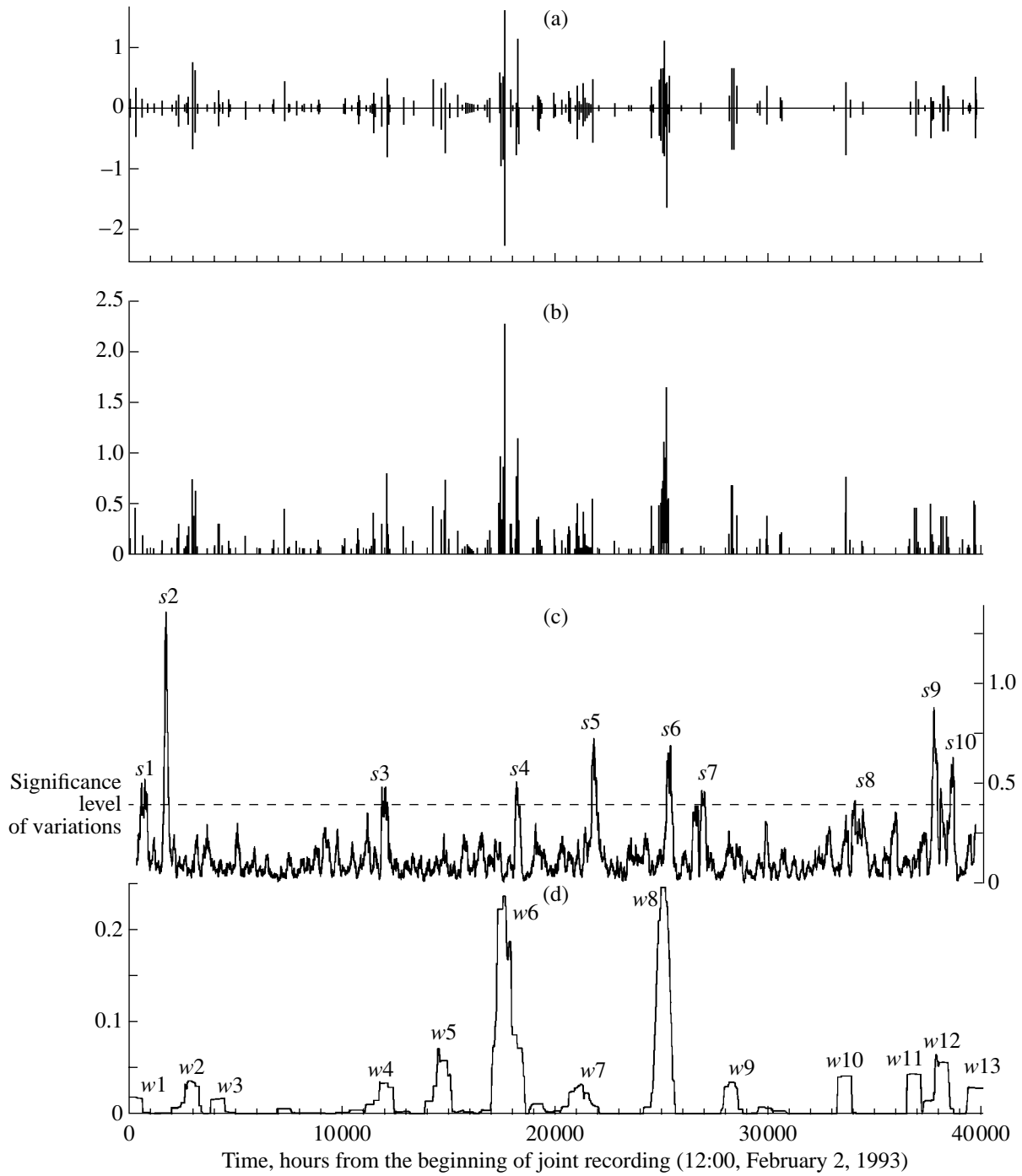


Fig. 3. (a) Plot of the wavelet-aggregated signal after the shrinkage of its wavelet coefficients at the first six detail levels with a 99% threshold and elimination of the higher detail levels (7 to 16); (b) ordinate moduli of the plot in Fig. 3a; (c) nonstationarity measure evolution of the high-frequency (periods shorter than 50 hours) component of the Fourier-aggregated signal in a moving time window of a 336-hour radius; (d) result of averaging of the plot in Fig. 3b over a moving time window of a 336-hour radius.

aging of periodograms over neighboring frequencies in the ordinary Fourier analysis):

$$\langle |c^{(\alpha)}(\tau_j^{(\alpha)})| \rangle = \frac{1}{2n^{(\alpha)}(\tau_{av}) + 1} \sum_{k=-n^{(\alpha)}(\tau_{av})}^{k=+n^{(\alpha)}(\tau_{av})} |c^{(\alpha)}(\tau_{j+k}^{(\alpha)})|, \quad (8)$$

where $n^{(\alpha)}(\tau_{av}) = \left\{ \frac{\tau_{av}}{\Delta t 2^\alpha} \right\}$ is an integer part of a number.

Therefore, at a sufficiently high detail level α (i.e., at sufficiently low frequencies of variations), $n^{(\alpha)}(\tau_{av})$ vanishes, and wavelet coefficients are not averaged. Absolute values of the coefficients are averaged in a time

Data on the most significant slow events

Number of event	Number of hours from 12:00 February 2, 1993 for the center of time window	Date of the event, the center of time window 672 hours wide
1	736	03:00 Mar. 5, 1993
2	1745	04:00 April 16, 1993
3	12076	15:00 June 20, 1994
4	18207	02:00 Mar. 3, 1995
5	21819	14:00 July 31, 1995
6	25418	13:00 Dec. 28, 1995
7	26905	12:00 Feb. 28, 1996
8	34107	14:00 Dec. 24, 1996
9	37775	10:00 May 29, 1997
10	38623	17:00 July 3, 1997

neighborhood of a current point. The length of this averaging neighborhood depends on the averaging parameter τ_{av} and the wavelet order (i.e., the length of its carrier at the current detail level). The midpoints of averaging neighborhoods having a radius of 128 samples (hours), $\tau_{av} = 128$, are plotted on the horizontal axes in Figs. 2b–2i. This value of the radius implies that the averaging was performed over neighboring values in moving neighborhoods of radii of 64, 32, 16, 8, 2, and 1 at respective detail levels of 1, 2, 3, 4, 5, and 6. The higher detail levels were not averaged.

The plots in Figs. 2b–2i exhibit maximums exceeding the background of neighboring statistical fluctuations. Note that these maximums tend to group. Certain groups of maximums exist simultaneously at all scale levels, and others, only at some levels shown in Fig. 2. The time intervals of grouping maximums (their characteristic length is about 1000 hours) fix the sought-for anomalies in the collective behavior of the time series analyzed. One can try to visually recognize the anomalies in Figs. 2b–2i, but this procedure encounter subjective difficulties that are overcome below by using a formal procedure based on the shrinkage operation (6).

The application of the shrinkage procedure (6) allows one to formalize the determination of anomalous intervals in terms of the wavelet analysis. For this purpose, the coefficients in the aggregated signal expansion were first set equal to zero at high detail levels ranging from 7 to 16. The shrinkage operation was then independently applied to the remaining six scale levels (variations on scales of no more than 64 h) with the parameter $\gamma = 0.99$ (only 1% of wavelet coefficients that are largest in modulus was left at each of the first six detail levels). The inverse transform of the “surviving” wavelet coefficients is shown in Fig. 3a, and its absolute values are plotted in Fig. 3b. Figure 3b is seen

to present a sequence of events (pulses) against the background of long intervals of zero values.

The plot in Fig. 3c shows the nonstationarity measure evolution of the high-frequency component in the Fourier-aggregated signal of the same four time series complemented to the end of the observations. As in the work [Lyubushin *et al.*, 1999], a double window of 672 hours (28 days) in width and an autoregression model of the 8th order were used, and preliminary operations were conducted to suppress the low-frequency component of the aggregated signal (at periods longer than 50 hours) and to “regularize” the spectrum. Details of the procedure together with considerations concerning the choice of the window width, autoregression order, and significance level of the variations (0.4) shown by a horizontally dashed line in Fig. 3c are given in [Lyubushin *et al.*, 1999].

An anomaly of the slow-event type means structural rearrangement in the spectral behavior at relatively high frequencies that occurs simultaneously in all processes recorded. If observations are made with a monitoring network covering a considerable region of the Earth’s crust, this rearrangement can indicate intensification of the tectonic energy dissipation in the upper crust, which manifests itself as more intense creep motions, landslide processes, and groundwater migration.

The table presents information on ten slow events associated with variations in the nonstationarity measure that exceed a significance level of 0.4. The events numbered in the table are referred to, respectively, as s_1 to s_{10} at the nonstationarity measure peaks in Fig. 3c.

Figure 3d is the result of averaging of the plot in Fig. 3b over a moving time window with a radius of 336 hours. This value is the same as the window width used for estimating the nonstationarity measure evolution in Fig. 3c. The averaging of the peaks in Fig. 3b produces 13 intervals (denoted, respectively, as w_1 to w_{13} in Fig. 3d) in which the averaging results essentially differ from zero. Now, the anomalous time intervals in the collective behavior of the analyzed time series inferred from the Fourier (s_1, \dots, s_{10}) and wavelet (w_1, \dots, w_{13}) analyses can be compared.

First, note that several of these anomalies correlate with one another in their occurrence time (e.g., w_1-s_1 , w_4-s_3 , w_6-s_4 , w_7-s_5 , w_8-s_6 , and $w_{10}-s_8$). The pair (w_{11}, w_{12}) correlate with the pair (s_9, s_{10}). The w anomalies usually precede the s anomalies by 500–1000 hours. The anomalies s_2 (most intense), s_7 , w_2 , w_9 , and w_{13} are autonomous (the latter may precede an s anomaly that was not discovered due to the stop in the joint measurements).

Thus, two types of anomalies can be introduced: the s -type (a slow event) and the w -type (a simultaneous increase in the amplitude of sharp small-scale varia-

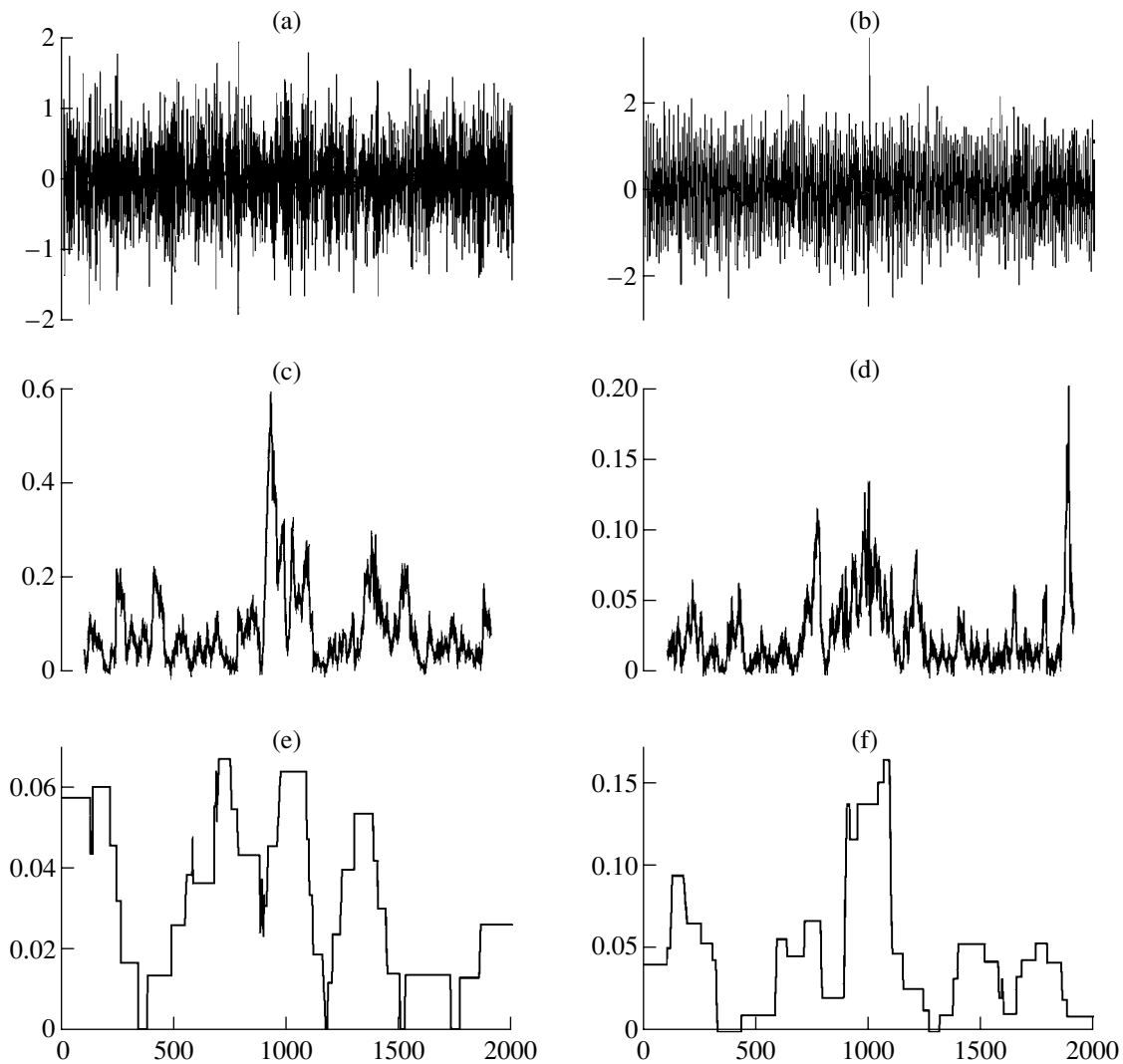


Fig. 4. Results of processing synthetic signals 2000 samples long. (a) Autoregression process of the first order ($a_1 = 0.5$, $s = 0.5$) + a sinusoid 40 samples long of a unit amplitude with a period of 4 samples introduced at the center of the series, $981 \leq t \leq 1020$; (b) sinusoid of a unit amplitude with a period of 10 samples + Gaussian white noise with the standard deviation $s = 0.5$ + Haar impulse: 0 for $t < 996$ and $t > 1004$, 1.5 for $996 \leq t \leq 1000$, and 1.5 for $1001 \leq t \leq 1004$; (c, d) plots of the nonstationarity measure evolution for signals (a) and (b), respectively, estimated in a moving time window of a 100-sample radius (autoregression of the first order); (e, f) anomalous time intervals identified with the use of wavelet filtering applied to signals (a) and (b), respectively (detail levels 5 through 11 were eliminated), the 99%-threshold shrinkage was separately applied to each of the first four detail levels, and the resulting moduli were averaged over a moving time window of a 100-sample radius.

tions in all of the processes analyzed). Below, I often an interpretation of these anomalies.

DISCUSSION AND CONCLUSIONS

A new method of joint analysis of time series obtained from monitoring systems is proposed. Its aim is to recognize an increase in the intensity of jumps that occurs simultaneously in the processes studied. The method is based on the construction of wavelet-aggregated signals previously proposed by the author. Characteristic features of the geophysical signals considered in this paper are interesting from the standpoint of the

search for hidden processes of enhancement in the fracture of geomaterials and an increase in the velocities of motion on the boundaries of crustal blocks.

The application of the method is exemplified by the analysis of four-dimensional time series of groundwater level variations measured in various aquifers in the Moscow region. The inferred anomalies of an increasing intensity of jumps are compared with anomalies of the slow-event type previously recognized from the same data. The jump intensity maximums correlate with slow events in eight out of ten cases and usually precede these events.

The principal difference between the method proposed in this paper and the previously developed method of slow events lies in the basis functions in use: they are harmonic in the Fourier analysis, whereas the Haar basis used in this paper is represented by finite step functions. In both cases, the aggregation procedure seeks a common signal that occur simultaneously in all scalar time series. This common signal can be rather strong (e.g., tidal variations in the groundwater level or their seasonal component), or it can be weak, "sunk" in local noise. The search for weak hidden common signals is most interesting. Varying the types of basis functions used in the aggregation procedure, one can recognize common signals of various classes.

Whereas the slow event is a hidden anomaly characterized by a fast change in the frequency composition of a weak common signal (obtained through an expansion in harmonics), an intensity peak of the wavelet-aggregated signal jumps (using the Haar basis upon application of the shrinkage procedure) means an increase in the intensity of sharp variations (jumps that can have small amplitudes and be hidden in individual noise) that occurs simultaneously in all processes. Since harmonics poorly suit the approximation of jumps (the well-known Gibbs phenomenon in the theory of Fourier series), the use of the Haar basis is *a fortiori* advantageous to the search for jumplike components.

The presence of jumplike components unrelated to defects in measurements or recording systems was repeatedly noted during observations of strains and groundwater level variations. Various hypotheses of the origin of jumplike signals can be proposed: for example, the relaxation of low stresses in rocks (a type of microearthquake) or the discharge of gas bubbles from wells during level observations. In any case, these signals are interesting for a geophysicist, and especially, if they are synchronously observed at different points of observation. The method proposed in the paper is intended for the recognition of precisely such a synchronous appearance of jumplike components in signals.

Methodologically, it is interesting to gain a deeper insight into the mechanism (from the standpoint of the signal structure) discriminating between the *s* and *w* anomalies. For this purpose, I conducted the following model experiment, whose results are presented in Fig. 4. Two synthetic signals 2000 samples long were generated. The first signal (Fig. 4a) was an autoregression process of the first order:

$$x(t) + a_1x(t-1) = \xi(t), \quad a_1 = 0.5, \quad \xi(t)$$

is the Gaussian white noise with the variance s^2 , $s = 0.5$.

A sinusoidal train 40 samples long with a unit amplitude and a period of 4 samples was introduced into this signal at the point $t = 981$ (i.e., was placed at

the center of the series). Thus, a spectral anomaly in the center of the sample was modeled.

The second synthetic signal (Fig. 4b) was a sinusoid of unit amplitude and a period of 10 samples including a Gaussian white noise (with a standard deviation of 0.5) and a jumplike anomaly in the form of a Haar impulse: 0 for $t < 996$ and $t > 1004$, -1.5 for $996 \leq t \leq 1000$, and 1.5 for $1001 \leq t \leq 1004$.

Figures 4b and 4c present the plots illustrating the nonstationarity measure evolution in signals 4a and 4b, respectively, estimated in a moving time window with a radius of 100 samples (autoregression of the first order). The modeled spectral anomaly in signal 4a is seen to be reliably identified as the maximum in Fig. 4c, whereas the Haar impulse is poorly resolved in Fig. 4d, the related peak not exceeding the background of neighboring statistical fluctuations.

Figures 4e and 4f present the plots of statistics used for the recognition of anomalous time intervals with the use of wavelet filtering of signals a and b, respectively. Here, the situation is opposite: the wavelet method ignores the spectral anomaly (Fig. 4e) but resolves the location of the hidden jumplike signal (Fig. 4f).

Note that the *w*-anomaly lead with respect to *s*-anomalies is interesting for studying the fine structure of background processes in the Earth's crust: in the majority of cases, a change in the spectral composition of the common signal is preceded by an increase in its jumplike component.

ACKNOWLEDGMENTS

This work was supported by the Russian Foundation for Basic Research, project no. 99-05-65175, and the International Association for the Promotion of Cooperation with Scientists from the Independent States of the Former Soviet Union, project no. 99-0099.

REFERENCES

- Chui, C.K., *An Introduction to Wavelets*, San Diego, CA: Academic, 1992.
- Daubechies, I., Orthonormal Bases of Compactly Supported Wavelets, *Commun. Pure Appl. Math.*, 1988, vol. 41, pp. 909–996.
- Daubechies, I., Ten Lectures on Wavelets, *CBMS-NSF Series in Applied Mathematics*, Philadelphia: SIAM, 1992, no. 61.
- Lyubushin, A.A., Jr., Multivariate Analysis of the Time Series of Geophysical Monitoring, *Fiz. Zemli*, 1993, no. 3, pp. 103–108.
- Lyubushin, A.A., Jr., Classification of the States of the Low-Frequency Geophysical Monitoring Systems, *Fiz. Zemli*, 1994, no. 7, pp. 135–141.
- Lyubushin, A.A., Jr., Analysis of Canonical Coherences in the Problems of Geophysical Monitoring, *Fiz. Zemli*, 1998a, no. 1, pp. 59–66.

- Lyubushin, Jr., A.A., An Aggregated Signal of the Low-Frequency Geophysical Monitoring Systems, *Fiz. Zemli*, 1998b, no. 3, pp. 69–74.
- Lyubushin, A.A., Jr., Analysis of Multidimensional Geophysical Monitoring Time Series for Earthquake Prediction, *Ann. Geofis.*, 1999, vol. 42, no. 5, pp. 927–937.
- Lyubushin, A.A., Jr., Wavelet-Aggregated Signal and Synchronous Pulsed Fluctuations in Problems of Geophysical Monitoring and Earthquake Prediction, *Fiz. Zemli*, 2000, no. 3, pp. 20–30.
- Lyubushin, A.A., Jr., Malugin, V.A., and Kazantseva, O.S., Monitoring of Tidal Variations of the Underground Water Level in a Group of Aquifers, *Fiz. Zemli*, 1997, no. 4, pp. 52–64.
- Lyubushin, A.A., Jr., Malugin, V.A., and Kazantseva, O.S., Recognition of “Slow Events” in an Aseismic Region, *Fiz. Zemli*, 1999, no. 3, pp. 35–44.
- Press, W.H., Flannery, B.P., Teukolsky, S.A., and Vetterling, W.T., *Numerical Recipes*, Cambridge: Cambridge Univ. Press, 1996, 2nd ed., ch. 13.